# Controlled Charge Switching on a Single Donor with a Scanning Tunneling Microscope

K. Teichmann, M. Wenderoth,* S. Loth, and R. G. Ulbrich
*IV. Physikalisches Institut, University of Göttingen, Friedrich-Hund-Platz 1, 37077 Göttingen, Germany*

J. K. Garleff, A. P. Wijnheijmer, and P. M. Koenraad
*Department of Semiconductor Physics, Eindhoven University of Technology, P.O. Box 513, NL-5600 MB Eindhoven, The Netherlands*
(Received 21 December 2007; published 15 August 2008)

The charge state of individually addressable impurities in semiconductor material was manipulated with a scanning tunneling microscope. The manipulation was fully controlled by the position of the tip and the voltage applied between tip and sample. The experiments were performed at low temperature on the {110} surface of silicon doped GaAs. Silicon donors up to 1 nm below the surface can be reversibly switched between their neutral and ionized state by the local potential induced by the tip. By using ultrasharp tips, the switching process occurs close enough to the impurity to be observed as a sharp circular feature surrounding the donor. By utilizing the controlled manipulation, we were able to map the Coulomb potential of a single donor at the semiconductor-vacuum interface.

DOI: 10.1103/PhysRevLett.101.076103 PACS numbers: 68.37.Ef, 73.20.Hb, 85.35.Gv

Nowadays both the research community and industry have a strong and increasing interest in the behavior of single impurities in semiconductor material. Commercial devices have reached the limit where single impurities can dominate the transport properties and where interfaces can affect the properties of impurities. For example in nanoscale devices Sellier *et al.* [1] investigated transport through single dopants in gated nanowires. Scanning tunneling microscopy (STM) is an excellent tool to probe and manipulate on this length scale. Wildöer *et al.* [2] showed that charges can be induced on a small grain by the STM tip. Repp *et al.* [3] reported the manipulation of Au adatoms on a NaCl film, where they used a voltage pulse to switch between two geometric configurations, which was accompanied by a charge manipulation. In this Letter we report on the manipulation of single electrons on a single donor in a dynamic manner, which does not need a structural modification. We can consider this process as a pure ionization, closely resembling operational devices. This opens the possibility to study donor-donor interactions and to measure the binding energy of individual donors.

We will demonstrate this effect on the well-known system Si:GaAs, which has been studied by several groups [4–8]. Our system behaves the same at voltages far from 0 V [4–6] and we used this to identify the observed features to be Si donors. At negative voltages we observe Friedel oscillations [7] and at high positive voltages the donors are positively ionized. The extra positive charge causes the bands to drop and results in an enhanced tunnel current, which is visualized in STM by a protrusion in the topography images. In contrast to the measurements presented in Refs. [4–8], we observe an extra feature. At relatively low positive voltages we observe sharp circular features around the donors, that we ascribe to the ionization of the donor due to the tip induced band bending (TIBB). In Si doped GaAs with a doping concentration $n_{\mathrm{Si}} \approx 10^{18}$ cm$^{-3}$ one finds that the lateral extension of the TIBB is of the same order as the radius of the tip apex [9]. For studying the ionization process, the lateral extension of the TIBB needs to be in the order of a few nanometer and therefore ultrasharp tips are needed.

We use electrochemically etched tungsten tips [10], which are glowed at ~1300 K. Afterwards the tips are sputtered by argon in ultrahigh vacuum, with a base pressure of $10^{-10}$ mbar. By this procedure we obtain clean, stable and ultrasharp tips, with a radius of curvature of the tip apex of a few nanometers, verified by scanning electron microscopy images. The measurements are performed at low temperature (LT), with two setups: a homebuilt LT STM and an Omicron LT STM.

Figure 1(a) shows a constant current topography image at 2 V and 100 pA. The donors are identified by their topographic contrast at negative voltages, where Friedel oscillations appear [7,8], as well as by spectroscopic be-

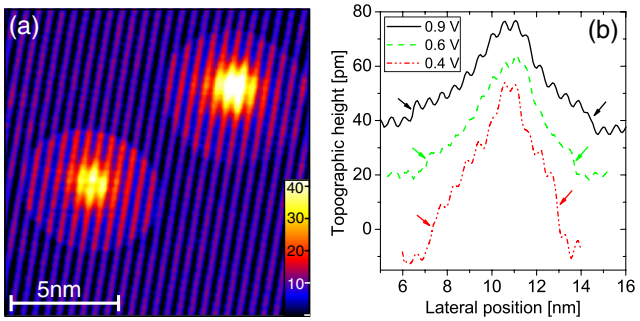


FIG. 1 (color online). (a) Shows a constant current topography image at 2 V and 100 pA. Two donors are surrounded by a disk of enhanced topographic height. The atomic corrugation is not disturbed by the disks. In (b) cross sections through another donor at different voltages are shown. At the edge of the disk a jump in the topographic height is seen, indicated by the arrows.

 

havior at positive and negative voltages. In contrast to former measurements on Si donors in GaAs, a disk of enhanced topographic height is visible around the donor. The atomic corrugation is not disturbed by the disk. The size of the disk depends on the applied voltage, as shown in Fig. 1(b). The topographic section shows that the edge of the disk appears as an instantaneous step, indicated by the arrows in Fig. 1(b). The width of the step is $<0.5$ Å, indicating that the disk is not related to local density of states effects. We will show that the step in the topography images is due to ionization of the donor.

We start our discussion with the description of the ionization mechanism, which is schematically shown in Fig. 2. When the tip is laterally far away from the donor [Fig. 2(a)], the bands on top of the donors are flat and are not influenced by the tip [Fig. 2(b)]. Since the measurements are done at 5 K, the thermal energy is much smaller than the ionization energy and the donors are neutral. If the tip is close to the donor [Fig. 2(c)], the bands are lifted at positive sample bias [Fig. 2(d)], and the donor level is pulled up as well. When the donor level is pulled above the onset of the conduction band in the bulk, the electron tunnels into the conduction band [Fig. 2(d)]. The Coulomb field of the ionized donor causes the bands at the surface to drop; therefore, the amount of states available for tunneling is enhanced. This results in an instantaneous enhancement of the tunnel current, leading to a retraction of the tip, as seen in Fig. 1(b). A similar feature was reported for a different system by Pradhan *et al.* [11].

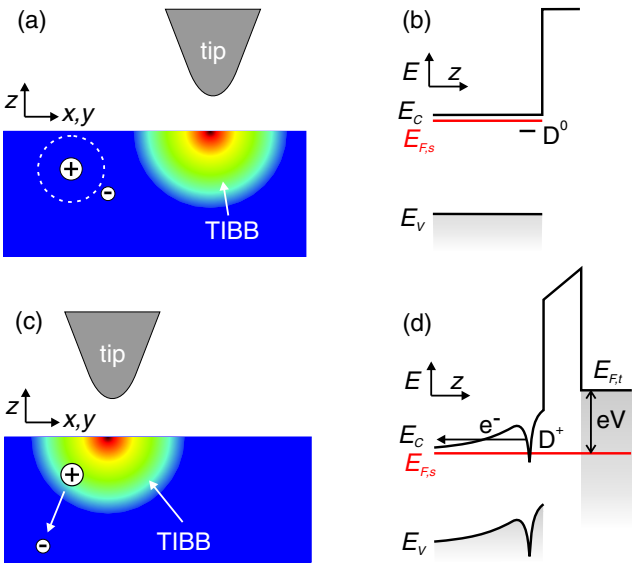


FIG. 2 (color online). Schematic representation of the ionization mechanism. When the tip is laterally far away from the donor (a), the bands on top of the donors are flat (b) and the donor will be neutral. As the tip approaches the donor with a positive sample bias (c), the bands are lifted due to the TIBB (d). When the donor level aligns with the conduction band in the bulk, the electron escapes.

The ionization process depends on the TIBB on top of the donor, which can be manipulated in three different manners: (i) changing the radial distance between the tip and the donor, simply by moving the tip laterally; (ii) increasing the applied voltage, which enhances the TIBB. At sufficiently low voltage the donor is neutral, and above a threshold voltage it is ionized; (iii) reducing the tip sample distance, which also enhances the TIBB. All three methods have been experimentally explored in detail and quantitatively agree with our calculations.

The ionization by laterally approaching the donor can be seen in constant current topography images. The edge of the disk in Fig. 1(a) represents the ionization of the donor. The disk diameter depends on the depth of the donor below the surface [12].

The proposed ionization mechanism predicts larger disks for higher tip sample voltages, which was experimentally investigated and confirmed by voltage dependent topography images and spatially resolved spectroscopy (STS). Figure 3(a) shows the topography image of the STS data set shown in Figs. 3(b)–3(d). In the differential conductance images the edge of the disk appears as a ring. Figures 3(b) and 3(c) show such a ring measured at 1.9 and 2.2 V, respectively. The images confirm that the diameter increases with voltage. Figure 3(d) shows a cross section through the spectroscopy map along the dashed line in 3(a). The hyperbola of higher differential conductivity corresponds to the diameter of the ring as a function of voltage. According to the proposed mechanism the donor ionizes at a certain TIBB; therefore, we expect the ring to follow a line with constant TIBB.

The contour lines of the calculated TIBB are added to the images 3(d) and 3(e), where we used the procedure described in Ref. [9] to calculate the TIBB in 3D. To extract the flatband condition, which is an essential parameter, we measured the effective barrier height simultaneously with the STS data [13]. For the data set shown in Figs. 3(a)–3(d) we found the flat band condition at 0.1 V. For another measurement [Fig. 3(e)] the flatband condition occurred at $-1.0$ V. Different flatband conditions stem from the range of observed tip work functions. The work function of bulk tungsten strongly differs if the surface is not perfectly flat [14,15]. For the measurement shown in Figs. 3(a)–3(d) the ring follows a calculated TIBB of $(180 \pm 50)$ meV and for the measurement shown in 3(e) the ring follows a calculated TIBB of $(150 \pm 50)$ meV. The TIBB calculations strongly depend on the tip sample distance, the tip shape, the flatband condition, and the (local) doping concentration. Some of these input parameters are unfortunately not known accurately in STM experiments. Within the range of reasonable values no unique fit can be found, due to correlations in the parameter space. This range of possible TIBB values results in the uncertainty of $\pm 50$ meV.

As a next step we changed the TIBB on top of the donor by varying the tip sample distance. The experimental result

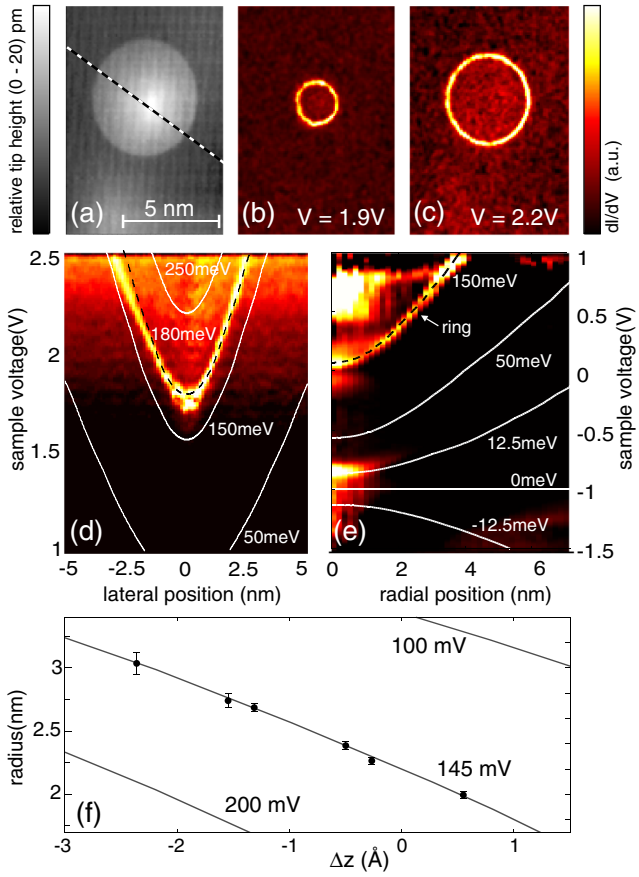


FIG. 3 (color online). (a) Topography image of a donor at a voltage of 2.5 V and current 500 pA. The dashed line indicates the position of the spectrum section in (d). (b),(c) Spatially resolved $dI/dV$ maps at different voltages. Higher differential conductivity is seen as a ring around the donor center, the ring diameter increase with voltage. (d) Shows a $dI/dV$ section along the dashed line in (a). The hyperbola corresponds to the ring in (b) and (c). A second measurement, acquired with a different tip, is shown in (e), where we averaged in angular direction. Contour lines of constant TIBB are added in both images. The details of the fitting are given in the text. (f) The measured position of the ring (dots) as a function of current setpoint and calculated contour lines of the TIBB.

is shown in Fig. 3(f). The disk diameter was extracted from topography images, where the current setpoint was varied from 5 pA to 3 nA, while the bias voltage was kept constant at 0.4 V. To convert the current setpoint into a tip sample distance, we used the exponential dependence $I \propto \exp(-2\kappa\Delta z)$. In good agreement with the literature [16], $\kappa$ was measured at $(1.10 \pm 0.04)$ Å$^{-1}$. The resulting variation of the tip sample distance is almost 3 Å in our experiment. Again, we performed TIBB calculations to quantitatively check the experimental disk diameters. In order to make this analysis the absolute distance between tip and sample ($z_{\mathrm{tip}}$) has to be known, but in STM only the relative change $\Delta z$ is known accurately. We assumed a typical tip sample distance of 5 Å at 20 pA and 0.4 V [16–18]. This corresponds to $\Delta z = 0$ Å in Fig. 3(f). Varying this value leads to a horizontal shift of the data points in Fig. 3(f) with respect to the calculated lines. The measurements are performed on exactly the same donor and with the same tip as the spectroscopy measurement shown in Fig. 3(e). With the same set of parameters as found to fit the voltage dependence of the ring diameter in Fig. 3(e), we find that the ring follows a calculated TIBB of 145 meV, which is very close to the value of 150 meV found for the voltage dependence measurement. The good agreement between both approaches supports the proposed ionization mechanism.

We use the steps in the tunnel current in the STS data to obtain detailed spatial information of the donor's electrostatic potential. The Coulomb potential of a single atomic charge $e^+$ is mapped with Å resolution. In Fig. 4(a) spectra on the free surface (solid line) are compared with spectra taken on top of a donor (dotted line). All spectra are normalized to a flat plane [10] to remove any crosstalk from the topographic contrast of the donor. In the spectrum taken directly on top of the donor a sharp current jump is visible at about 1.3 V which is caused by the ionization of

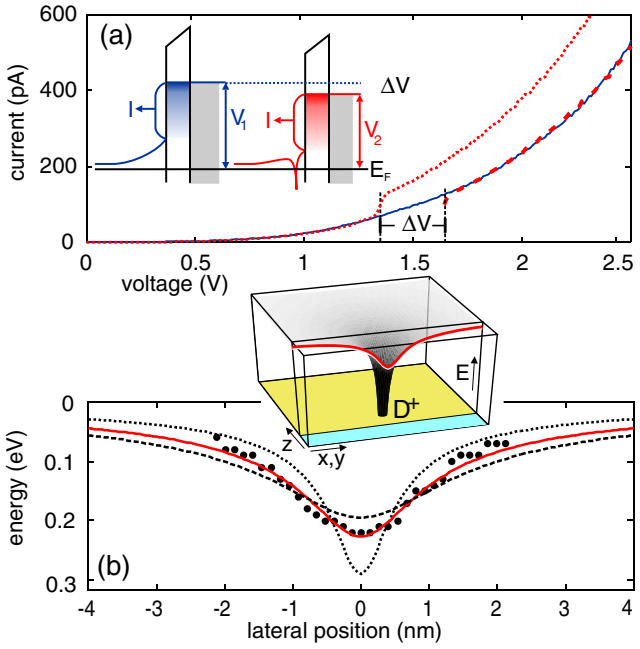


FIG. 4 (color online). A spectrum taken directly above the donor (dotted line) and on the free surface (solid line) are shown in (a). At voltages lower than 1.3 V the curves overlap. The curves overlap for higher voltages as well, by shifting the spectrum above the donor by a certain voltage (dashed line). The situation is schematically shown in the upper inset. The voltage shift directly gives the Coulomb potential originating from the ionized donor. We measured the voltage shift for different lateral distances to the donor center. The results are the dots in (b). The data are fitted with the Coulomb potential directly at the surface; see solid line in the lower inset. The three curves correspond to different donor depths, given in the text.

the donor. At voltages below 1.3 V the curves overlap. For higher voltages the ionized donor gives rise to an enhanced current. This is schematically shown in the inset of Fig. 4(a). We assume that the ionized donor pulls down the bands, which enhances the number of states available for tunneling, and thus enhances the tunnel current, compared to the free surface. On the free surface a higher voltage $V_1$ is needed to obtain the same amount of available states for tunneling, which results in the same amount of current $I$. Therefore the data curve after the jump is manually shifted by a certain voltage, $\Delta V$, until the current is the same (dashed line). The two curves overlap perfectly for higher voltages. This voltage shift directly gives the Coulomb potential originating from the ionized donor. We measured the voltage shift, with the same procedure, as a function of distance to the donor center. The dots in Fig. 4(b) are the measured voltage shift. The measured voltage shift is the potential of the donor directly at the surface, which is illustrated with the solid line in the inset of Fig. 4(b). The potential of a charge which is near an interface of a dielectric and the vacuum can be solved analytically with an electrostatic approach using image charges [19]. According to this solution the potential directly at the interface should behave like a Coulomb potential, with a modified dielectric constant $\epsilon_{r,\mathrm{eff}} = (\epsilon_{r,\mathrm{vac}} + \epsilon_{r,\mathrm{GaAs}})/(2\epsilon_{r,\mathrm{vac}})$. In GaAs the bulk value of $\epsilon_r = 13.1$ [20], we would expect to find a value of about 7. Therefore we determined the fitted Coulomb potential by the depth of the donor below the surface and $\epsilon_r$, which can be extracted independently. Additionally, a topographic image taken on this donor at negative voltages was used to determine that the donor is in an even layer [4,21]. The depth of the donor below the surface thus has to be a multiple of the *double* layer thickness, 4 Å. The fitting process was done for $\epsilon_r$ and for a donor in three different even monolayers. Figure 4(b) presents the best fit for a donor 4 Å below the surface (dotted line) with an $\epsilon_r = 12.4$, a donor 8 Å below the surface (solid line) with an $\epsilon_r = 8$, and a donor 12 Å below the surface (dashed line) with an $\epsilon_r = 6.2$. The best correlation was obtained for a donor depth of 4 monolayers. The measurement was performed on three different donors. In all measurements the value of $\epsilon_r$ for the best fit was $(8 \pm 1)$. This is close to the expected value following the classical half-space approach.

We have shown that the charge state of individual donors can be precisely controlled by STM in a dynamic manner. The dependence of the ring diameter on the voltage and the current setpoint proves that the donor state can be ionized by moving the tip laterally, enhancing the voltage or reducing the tip sample distance. We use this ionization process to measure the Coulomb potential originating from a single ionized donor, which further validates the proposed ionization mechanism. Manipulating the charge of individual donors opens new possibilities, e.g., studying donor-donor interactions and measuring the binding energy of individual donors.

We thank Peter Maksym, Mervyn Roy, Felix Marczinowski, and Jens Wiebe for valuable discussions, and DFG-SFB 602 A7, DFG-SPP 1285, the German National academic foundation, ASPRINT, and STW-VICI grant 6631 for financial support.

*wenderoth@ph4.physik.uni-goettingen.de

[1] H. Sellier *et al.*, Phys. Rev. Lett. **97**, 206805 (2006).
[2] J. W. G. Wildöer *et al.*, Phys. Rev. B **53**, 10 695 (1996).
[3] J. Repp *et al.*, Science **305**, 493 (2004).
[4] J. F. Zheng *et al.*, Phys. Rev. Lett. **72**, 1490 (1994).
[5] D. Stievenard, Mater. Sci. Eng. B **71**, 120 (2000).
[6] R. M. Feenstra *et al.*, Phys. Rev. B **66**, 165204 (2002).
[7] M. C. M. M. van der Wielen, A. J. A. van Roij, and H. van Kempen, Phys. Rev. Lett. **76**, 1075 (1996).
[8] M. Wenderoth *et al.*, Europhys. Lett. **45**, 579 (1999).
[9] R. M. Feenstra, J. Vac. Sci. Technol. B **21**, 2080 (2003).
[10] J. K. Garleff *et al.*, Phys. Rev. B **70**, 245424 (2004).
[11] N. A. Pradhan *et al.*, Phys. Rev. Lett. **94**, 076801 (2005).
[12] A. P. Wijnheijmer *et al.* (to be published).
[13] S. Loth *et al.*, Phys. Rev. B **76**, 235318 (2007).
[14] K. Besocke and H. Wagner, Phys. Rev. B **8**, 4597 (1973).
[15] P. Hahn, J. Clabes, and M. Henzler, J. Appl. Phys. **51**, 2079 (1980).
[16] R. M. Feenstra and J. A. Stroscio, J. Vac. Sci. Technol. B **5**, 923 (1987).
[17] C. J. Chen and R. J. Hamers, J. Vac. Sci. Technol. B **9**, 503 (1991).
[18] J. K. Garleff *et al.*, Phys. Rev. B **76**, 125322 (2007).
[19] J. D. Jackson, *Classical Electrodynamics* (Wiley & Sons, New York, 1999).
[20] S. Adachi, *GaAs and Related Materials Bulk Semiconducting and Superlattice Properties* (World Scientific, Singapore, 1994).
[21] A. Depuydt *et al.*, Appl. Phys. A **72**, S209 (2001).